

Quantum size correction to the work function and the centroid of excess charge in positively ionized simple metal clusters

M Payami

Center for Theoretical Physics and Mathematics, Atomic Energy Organization of Iran, P. O. Box 11365-8486, Tehran, Iran

(Received 3 May 2003; accepted 27 October 2003)

Abstract

In this work, we have shown the important role of the finite-size correction to the work function in predicting the correct position of the centroid of excess charge in positively charged simple metal clusters with different r_s values ($2 \leq r_s \leq 7$). For this purpose, firstly we have calculated the self-consistent Kohn-Sham energies of neutral and singly-ionized clusters with sizes $2 \leq N \leq 100$ in the framework of local spin-density approximation and stabilized jellium model (SJM) as well as simple jellium model (JM) with rigid jellium. Secondly, we have fitted our results to the asymptotic ionization formulas both with and without the size correction to the work function. The results of fittings show that the formula containing the size correction predict a correct position of the centroid inside the jellium while the other predicts a false position, outside the jellium sphere.

Keywords: workfunction, centroid, cluster, Jellium, density functional theory

1. Introduction

In the SJM, [1] the total energy of a cluster with jellium radius $R = r_s^{-1/3} N^{1/3}$ is given by

$$E_R[n] = T_s[n] + E_{xc}[n] + \int d\mathbf{r} \left\{ \frac{1}{2} \phi_R([n]; \mathbf{r}) + \langle \delta v \rangle_{ws} \right. \quad (1)$$

$$\left. \Theta(\mathbf{r}) \right\} [n(\mathbf{r}) - n_+(\mathbf{r})] + (\varepsilon_M + \bar{\omega}_R) \int d\mathbf{r} n_+(\mathbf{r}).$$

The first and second terms on the right hand side of eq. (1) are the non-interacting kinetic and the exchange-correlation energies, respectively and we have

$$\phi_R([n]; \mathbf{r}) = \int d\mathbf{r}' \frac{n(\mathbf{r}') - n_+(\mathbf{r}')}{|\mathbf{r} - \mathbf{r}'|}. \quad (2)$$

All equations throughout this paper are in atomic units ($\hbar = e^2 = m = a_0 = 1$) unless otherwise explicitly expressed. $n_+(\mathbf{r})$ is the positive jellium background density, $n_+(\mathbf{r}) = \bar{n} \theta(R - r)$ where $\bar{n} = 3/4\pi r_s^3$ is the bulk density. The quantity $\langle \delta v \rangle_{ws}$ is [1] the average of the difference potential over the Wigner-Seitz cell and the difference potential, $\langle \delta v \rangle$, is defined as the

difference between the pseudo-potential of a lattice of ions and the electrostatic potential of the jellium positive background. $\Theta(\mathbf{r})$ takes the value of unity inside the jellium background and zero outside. ε_M and $\bar{\omega}_R$ are the Madelung energy and the repulsive part of the pseudo-potential, respectively.

In the continuum approximation, the ground-state density $n_R(\mathbf{r})$ of the neutral cluster is given by the solution of the Euler equation [2]

$$\mu(R) = \frac{\delta E_R[n]}{\delta n(\mathbf{r})} \Big|_{n=n_R} = \phi_R([n_R]; \mathbf{r}) \quad (3)$$

$$+ \langle \delta v \rangle_{ws} \Theta(\mathbf{r}) + \frac{\delta E_{kxc}[n]}{\delta n(\mathbf{r})} \Big|_{n=n_R}.$$

In eq. (3), $\mu(R)$, is the chemical potential of electrons which is constant throughout the cluster for the exact ground-state density n_R , and $E_{kxc} = T_s + E_{xc}$. The ground-state density satisfies the constraint $\int d\mathbf{r} n_R(\mathbf{r}) = N^*$. Removing an electron from the neutral cluster gives rise to a new ground-state density

$$n'_R(\mathbf{r}) = n_R(\mathbf{r}) + \delta n(\mathbf{r}) \text{ with } \int dr \delta n(\mathbf{r}) = -1.$$

The ionization energy is defined as the difference in the ground-state energies of the two systems with N^* and $(N^* - 1)$ electrons which may be represented by the expansion

$$\begin{aligned} I(R) &= E_R[n'_R] - E_R[n_R] \\ &= \int d\mathbf{r} \frac{\delta E_R[n]}{\delta n(\mathbf{r})} \Big|_{n=n_R} \delta n(\mathbf{r}) \\ &\quad + \frac{1}{2} \int d\mathbf{r} \int d\mathbf{r}' \frac{\delta^2 E_R[n]}{\delta n(\mathbf{r}) \delta n(\mathbf{r}')} \Big|_{n=n_R} \delta n(\mathbf{r}) \delta n(\mathbf{r}') + \dots \end{aligned} \quad (4)$$

The first term on the right hand side of eq. (4) is $-\mu(R)$ and in local density approximation for the kinetic and exchange-correlation energies we have

$$\begin{aligned} \frac{\delta^2 E_R[n]}{\delta n(\mathbf{r}) \delta n(\mathbf{r}')} \Big|_{n=n_R} &= \frac{1}{|\mathbf{r} - \mathbf{r}'|} + \\ &\delta(\mathbf{r} - \mathbf{r}') \frac{\partial^2}{\partial n^2} \{n \varepsilon_{kxc}(n)\} \Big|_{n=n_R} \end{aligned} \quad (5)$$

Here, $\varepsilon_{kxc}(n)$ is the sum of the bulk kinetic and exchange-correlation energies per electron at the density n . Choosing a spherical distribution [3] for $\delta n(\mathbf{r})$

$$\delta n(\mathbf{r}) = \frac{\zeta(r)}{4\pi(R+a)^2}, \quad (6)$$

and interpreting $(R+a)$ as the centroid of the excess charge, $\zeta(r)$ satisfies the following two equations:

$$\int_0^\infty \frac{\zeta(r)}{4\pi(R+a)^2} 4\pi r^2 dr = -1, \quad (7)$$

$$\int_0^\infty r \frac{\zeta(r)}{4\pi(R+a)^2} 4\pi r^2 dr = -(R+a). \quad (8)$$

The simplest choice for $\zeta(r)$ which satisfies the above two constraints, is

$$\zeta(r) = -\delta(r - R - a). \quad (9)$$

Using the eqs. (5)-(9) in the second term of the right hand side of the eq. (4) one obtains

$$I(R) = -\mu(R) + \frac{1}{2(R+a)} + O(R^{-2}). \quad (10)$$

Since $\mu(R)$ is a constant, independent of \mathbf{r} , for the exact ground-state density of the neutral cluster, $n_R(\mathbf{r})$, it is possible to evaluate it at a point deep inside the cluster where $n_R(\mathbf{r}) = \bar{n}$. The density profile $n_R(r)$ and the potential $\phi_R([n_R], r)$ for large clusters can be expressed as corresponding quantities for the planar surface (i.e. $R = \infty$) plus a size correction [4]

$$n_R(x) = n(x) + \frac{f(x)}{R} + O(R^{-2}), \quad (11)$$

$$\phi_R(x) = \phi(x) + \frac{h(x)}{R} + O(R^{-2}), \quad (12)$$

where $x = r - R$ gives the distance from the jellium edge. At large distances from the jellium edge outside the cluster, we have $f(+\infty) = \phi(+\infty) = h(+\infty) = 0$, and for a point deep inside the cluster ($x = -\infty$) we have $n(-\infty) = \bar{n}$, $f(-\infty) = 0$. Hence eq. (3) reads

$$\mu(R) = \phi(-\infty) + \frac{h(-\infty)}{R} + \langle \delta v \rangle_{ws} + \frac{\partial}{\partial n} \{n \varepsilon_{kxc}(n)\} \Big|_{n=\bar{n}}. \quad (13)$$

Upon inserting eq. (13) into eq. (10) and using the definition of the work function of a planar surface in the SJM [5]

$$W = \Delta\phi - \langle \delta v \rangle_{ws} - \frac{\partial}{\partial n} \{n \varepsilon_{kxc}(n)\} \Big|_{n=\bar{n}}, \quad (14)$$

where $\Delta\phi = \phi(+\infty) - \phi(-\infty)$ is the electrostatic dipole barrier [6], one obtains

$$I(R) = (W + \frac{c}{R}) + \frac{1}{2(R+a)} + O(R^{-2}), \quad (15)$$

where $c = -h(-\infty)$.

Equation (15) is also valid in the JM for which W is obtained by putting $\langle \delta v \rangle_{ws} = 0$ in eq. (14) and recalculating $\Delta\phi$ with the JM density profile. There are two methods [7, 8, 5] for calculating W and c called the "Koopmans' method" and the "change in self-consistent field (ΔSCF) method" which give the same results for the correct $n(x)$ but the ΔSCF method has the advantage that its results are less sensitive to the exact density profile $n(x)$. However, in our calculations, all the quantities W , c , and a are obtained from fitting of our self-consistent ionization energies of the clusters to eq. (15).

2. Computational scheme and results

In this work, using the JM as well as the SJM with local spin-density approximation [9], we have solved the self-consistent Kohn-Sham equations [10] and obtained the energies of neutral and singly-ionized N -atomic clusters of different sizes ($2 \leq N \leq 100$). The calculations have been performed for different \bar{r}_s values of the jellium sphere ($2 \leq \bar{r}_s \leq 7$) in steps 0.5 bohr. For each \bar{r}_s value, we have calculated the ionization energies

$$I(R) = E_R(N-1) - E_R(N), \quad (16)$$

for $2 \leq N \leq 100$ with $R = N^{1/3} \bar{r}_s$. Then, by fitting the $I(R)$ values to eq. (10) we have obtained the values of W , c , and α for that \bar{r}_s value.

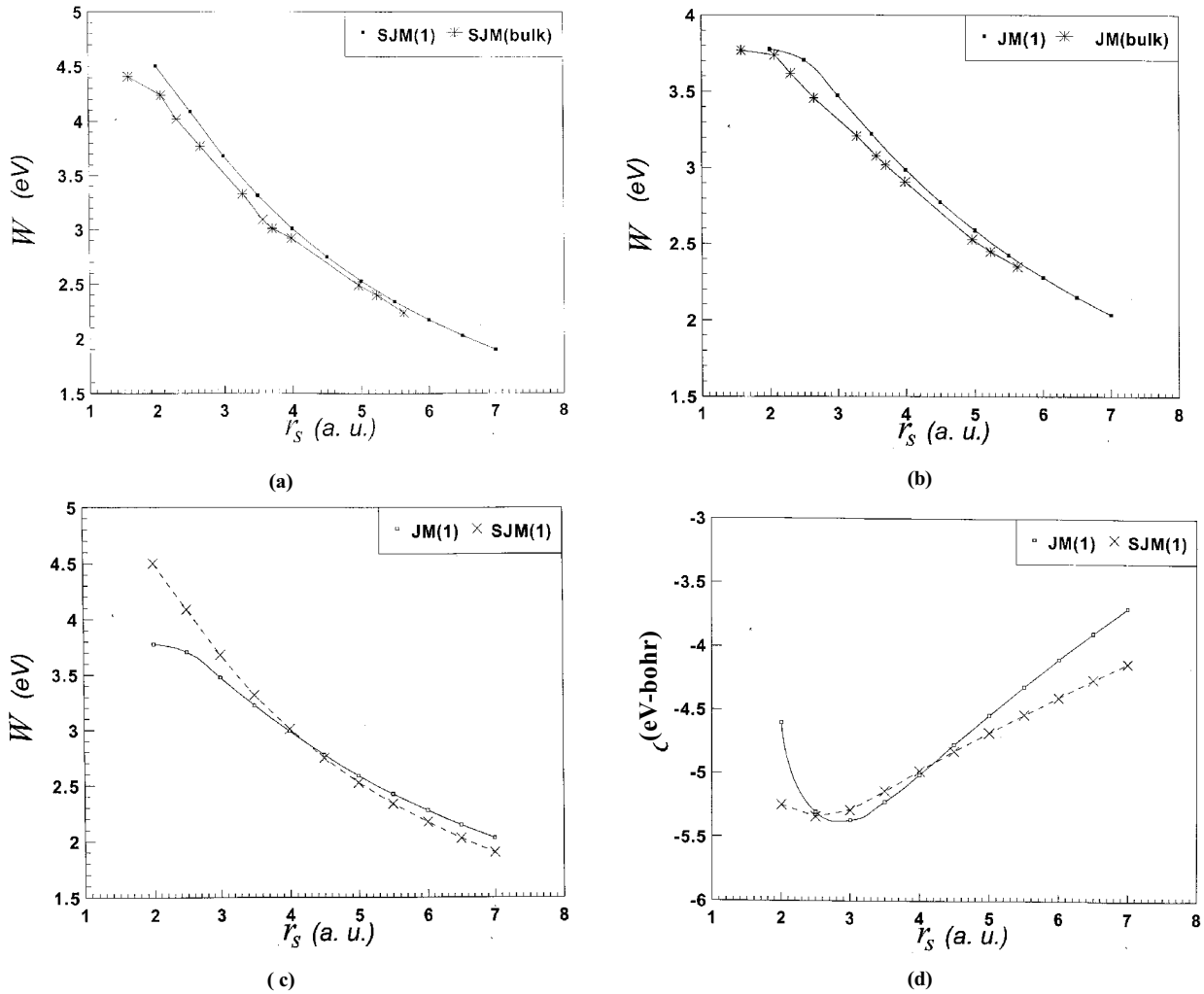


Figure 1. Work functions in eV and quantum size corrections in eV-bohr from scheme 1. In (a) - the fitted values of the work function has been compared with those of the bulk calculation for the SJM. (b) - the same as (a) but for the JM. (c) - compares the fitted JM and SJM work functions. (d) - compares the fitted quantum size corrections in the JM and the SJM.

Figure 1(a) shows the work function obtained for our SJM data and is labeled as SJM(1) because in this paper we have called the eq. (15) as scheme 1. To compare our results with the bulk calculation results, SJM(bulk), we have also plotted the data from table IV of Ref. [12]. As is seen, our results show a good agreement with the bulk calculations results.

In Figure 1(b) we have compared our JM(1) results with the bulk JM results of Ref. [12]. Here also the good agreement is obvious.

Figure 1(c) compares the JM(1) and the SJM(1) results. These two curves coincide at $\bar{r}_s \approx 4.18$ where the JM is mechanically stable. The difference $W_{\text{SJM}} - W_{\text{JM}}$ is positive for $\bar{r}_s < 4.18$ and changes sign for $\bar{r}_s > 4.18$. This behavior can easily be predicted if one resorts to the corresponding expressions for the work functions: For $\bar{r}_s \approx 4.18$, we have $\langle \delta v \rangle_{\text{ws}} \approx 0$ and

therefore, the density profiles are the same which results in $\Delta\phi[n_{\text{SJM}}] = \Delta\phi[n_{\text{JM}}]$ and in turn, by eq. (14) leads to the same workfunctions. However, since the term $\langle \delta v \rangle_{\text{ws}}$ in eq. (14) changes sign at $\bar{r}_s = 4.18$, it gives rise to the change in the sign of $W_{\text{SJM}} - W_{\text{JM}}$.

In Figure 1 (d), the values of the quantum size correction c for the JM(1) and the SJM(1) are compared. These two plots have two intersections. The one at $\bar{r}_s \approx 4.18$ is obvious if we consider the dependence [4,5] of the quantity c on the density profile $n(x)$

$$c = -h(-\infty) = \mp \pi \int_{-\infty}^{+\infty} dx \{x^{\mp} [n(x) - \bar{n}\theta(-x)] + xf(x)\}, \quad (17)$$

$$\int_{-\infty}^{+\infty} dx f(x) = -2 \int_{-\infty}^{+\infty} dx x [n(x) - \bar{n}\theta(-x)] \quad (18)$$

$$= -\frac{1}{2\pi} \Delta\phi. \quad (19)$$

The intersection at $\bar{r}_s \approx 2.5$ is because of the improper behavior of the properties at high densities in the JM (See for example figure 6(a) of Ref. [13] for the surface energy which becomes negative for $\bar{r}_s < 2.5$).

In figure. 2 (a), we have shown the position of the centroid of excess charge, a , for the singly-ionized clusters as a function of \bar{r}_s both for the JM(1) and the SJM(1). As is seen, both plots predict negative values which means that the centroid for a positively charged cluster lies inside the jellium [the jellium surface is taken as the origin, see eq. (6)]. This is consistent with our understanding that the excess charge in a metal resides on the surface. On the other hand, the JM(1) and the SJM(1) have opposite behaviors: the former is decreasing (increasing in absolute value) and the latter is increasing (decreasing in absolute value) and intersect each other at $\bar{r}_s \approx 4.18$. The explanation of these opposite behaviors is straightforward: In simple JM, if we take the thickness of the jellium shell at the edge as λ , then the volume of this shell contains a unit charge (for singly-ionized clusters)

$$\lambda(4\pi R^2)\bar{n} = 1, \quad (20)$$

which gives

$$a \approx -\frac{1}{2}\lambda = -\frac{1}{6R^2}\bar{r}_s^3. \quad (21)$$

By eq. (21), for a fixed R , in JM as \bar{r}_s increases, the position of the centroid moves inside from the edge towards the center of the jellium sphere. However, in the SJM, there exist two competing effects: On the one hand, as in the simple JM, because the jellium background is the same, increasing \bar{r}_s has the tendency to increase λ . On the other, the SJM Kohn-Sham effective potential contains an extra term $\langle \delta v \rangle_{ws}$ which is an increasing function of \bar{r}_s (See Table IV of Ref.[1]). This term is negative for $\bar{r}_s < 4.18$ and hence deepens the effective potential (compared to the JM) which reduces the spill-out of the electrons, so that $a_{SJM} < a_{JM}$. For $\bar{r}_s > 4.18$ the extra term is positive which shallows the effective potential (compared to the JM) which in turn increases the range of the Kohn-Sham orbitals from which the electron density is calculated. The result is that in the SJM, the overlap of the negative and positive charges increases (the shell thickness decreases) with increasing \bar{r}_s , so that $a_{SJM} > a_{JM}$.

The quantity a calculated above is, of course, the centroid position for singly-ionized cluster. To calculate the centroid position for doubly-ionized clusters, we fitted the Kohn-Sham energies of doubly-ionized clusters to the eq. (20) of Ref[5] which is obtained from Taylor expansion of the energy of a z -ply charged cluster about

$z=0$. The resulted values for a was +0.34, -0.18, -0.29 for \bar{r}_s values 2, 4, 6, respectively. Obviously, the result for $\bar{r}_s = 2$ is incorrect because of its wrong sign. The predicted value for $\bar{r}_s = 6$ is quite acceptable and consistent with the above arguments. One reason for the incorrect results may be in the use of Taylor expansion about $z=0$ for points $z \gg 0$, as in eq. (20) of Ref. [5]. A better approximation is obtained by using the z -th ionization energy

$$I_z(R) = E_R(N^* - z) - E_R(N^* - z + 1) \quad (22)$$

$$= -\epsilon_R^{HO}(N^* - z + 1) + \frac{1}{2(R + a_z)}, \quad (23)$$

where we have used the Taylor expansion of the ground-state energy $E_R(N^* - z)$ at $N^* - z + 1$. The quantity $\epsilon_R^{HO}(N^* - z + 1)$ is the highest occupied Kohn-Sham orbital energy [11] for the $(z-1)$ -ply ionized cluster with radius $R = \bar{r}_s(N^*)^{1/3}$.

It is instructive to compare the behaviors of the position of the centroid of excess charge with the position of the image plane of a planar surface. In figure. 2 (b) we have compared these quantities in the JM and the SJM. As is seen, both of them are positive and intersect at $\bar{r}_s \approx 4$. In the JM plot we have used the eq. (8) of Ref. [3] and for the SJM we have used the data from figure. 1 of Ref. [14]. Here, although the argument used for the finite cluster to calculate λ is useless, the effect of $\langle \delta v \rangle$ is the same as in the finite cluster case which leads to similar behaviors.

Now, we show the results of fitting our self-consistent Kohn-Sham energies to eq. (15) but neglecting the quantum size correction, as in eq. (16) of Ref. [3]. Putting $c=0$ in eq. (15) we call the resulting equation as scheme 2.

In figure. 3 (a) we have compared the work functions obtained in schemes 1 and 2. As is seen, the scheme 2 predicts lower values than the scheme 1 otherwise the shapes are the same.

Figure 3(b) shows the plots of a for JM and SJM in scheme 2. As we see, both of them are positive and have increasing behaviors. This means that the position of the centroid of the excess positive charge (for the singly-ionized clusters) lies outside the jellium edge which is incorrect because there exists no positive charge. Therefore, inclusion of the quantum size effect is vital for predicting correct values of the physical quantities.

Finally, we introduce scheme 3 which is obtained by putting $a=0$ in eq. (15) as eqs. (1) of Refs. [5] and [15]. In figure. 4 (a) we have compared the SJM work functions in schemes 1 and 3 with the bulk values [12]. It is seen that scheme 3 improves the work function and reduces the distance from the bulk values at higher densities.

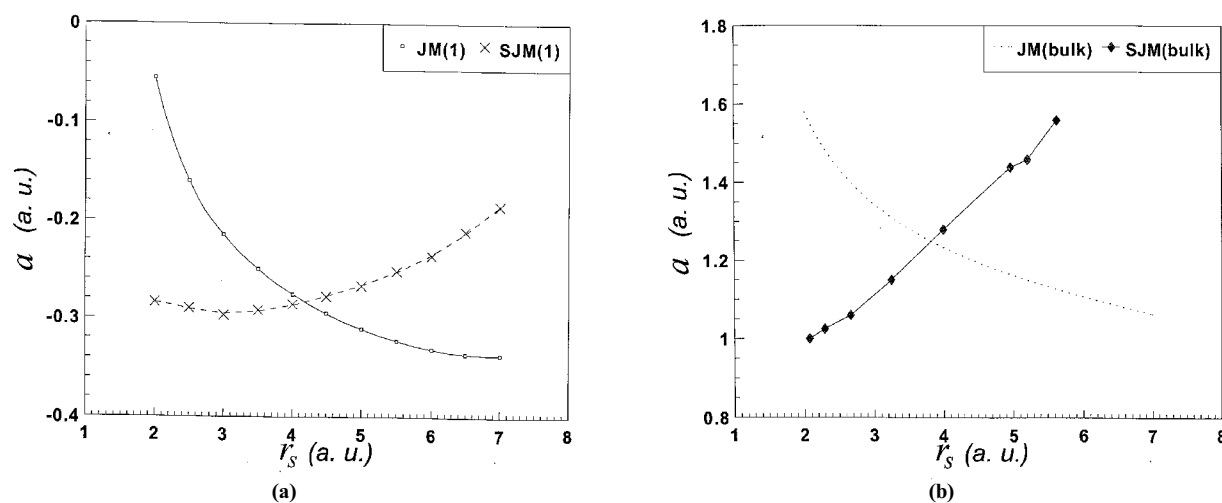


Figure 2. (a)- The scheme 1 positions of the centroid of excess charge, in atomic units, as functions of \bar{r}_s for the JM and the SJM. (b)- The positions of the image planes for the planar surfaces, in atomic units, from bulk calculations of the JM and the SJM

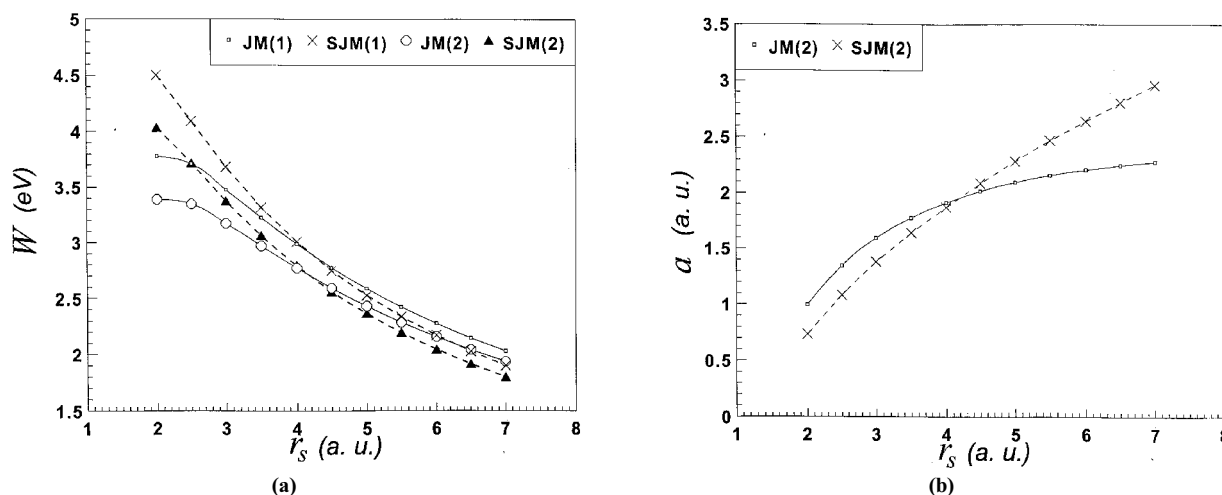


Figure 3. (a)- Work functions of schemes 1 and 2 in electron volts are compared. (b)- Position of the centroid of excess charge, in atomic units, in scheme 2. Both the SJM and the JM show increasing behaviors.

The SJM fitted values of the size correction for schemes 1 and 3 are compared in figure 4 (b). It is seen that in scheme 3, the values are nearly constant for the metallic densities $c \approx -3.7\text{eV}\cdot\text{bohr}$ in good agreement with the result of Ref. [5].

3. Summary and conclusions

We have calculated the self-consistent Kohn-Sham energies for neutral and singly-ionized clusters with different sizes and repeated the calculations for different \bar{r}_s values in the metallic range. The ionization energies for each \bar{r}_s has been separately fitted to eq. (15), we called scheme 1. The results obtained for the position of the centroid of excess charge is consistent with the understanding that excess charges reside at the outer surface of a metal particle. However, for small doubly-

ionized clusters, using the Taylor expansion about $z=0$ gives incorrect a values for clusters of high electron-density metals. A better result would be obtained by using a Taylor expansion of the energy of z -ply ionized cluster about the point $(z-1)$.

Next, in scheme 2, we have fitted the same ionization energies to eq. (15) taking $c=0$. The results show incorrect values for the centroid position.

Finally, in scheme 3, we put $a=0$ in eq. (15) and fit the ionization energies, which results in better values for the work function at higher densities.

To conclude, if one wishes to calculate the position of the centroid of excess charge of z -ply charged cluster, one should use the Taylor expansion about point $(z-1)$ as in eq. (23). On the other hand, if one wishes choose one of the versions of eq. (15) to calculate the ionization energies (or electron affinities) of simple metal clusters,

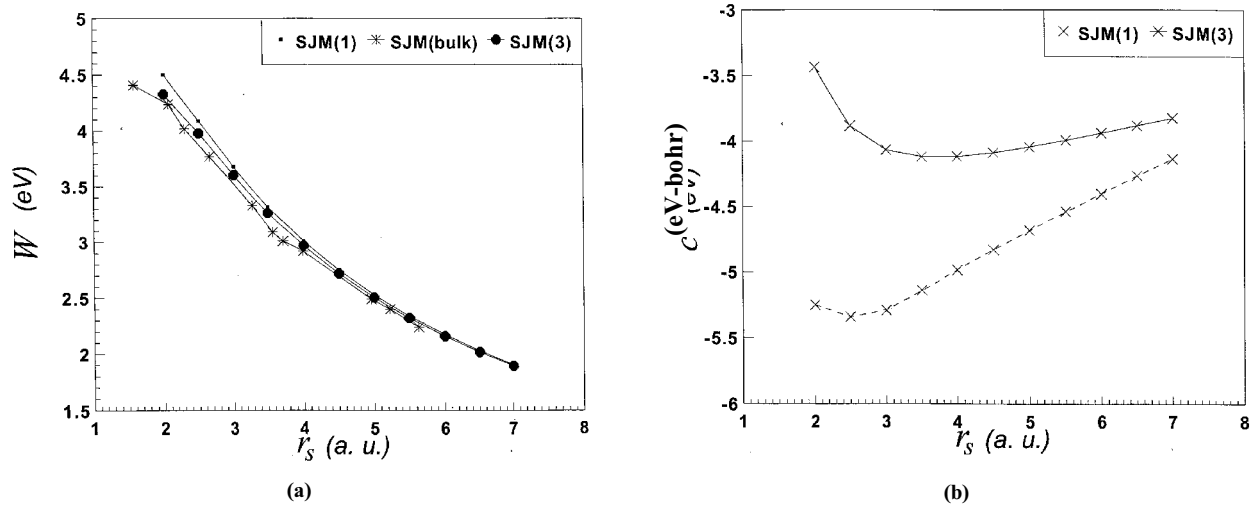


Figure 4. (a)- Work functions in electron volts for schemes 1 and 3 are compared with the bulk. (b) - quantum size corrections in eV-bohr for the schemes 1 and 3. The scheme 3 predicts more or less a constant value.

the best choice would be the eq. (15) with the ΔSCF values for W and c , and for sufficiently large clusters ($R \gg a$) the scheme 3 with the ΔSCF values for W and c gives the same results as scheme 2.

Reference

1. J P Perdew, H Q Tran and E D Smith, *Phys. Rev. B* **42** (1990) 11627.
2. R G Parr and W Yang, *Density-Functional Theory of Atoms and Molecules* (Oxford University Press 1989).
3. J P Perdew, *Phys. Rev. B* **37** (1988) 6175.
4. E Engel and J P Perdew, *Phys. Rev. B* **43** (1991) 1331.
5. M Seidl, J P Perdew, M Brajczewska and C Fiolhais, *J Chem. Phys.* **108** (1998) 8182.
6. N D Lang and W Kohn, *Phys. Rev. B* **1** (1970) 4555.
7. R Monnier, J P Perdew, D C Langreth and J W Wilkins, *Phys. Rev. B* **18** (1978) 656.
8. M Seidl and M Brack, *Ann. Phys.* **245** (1996) 275.
9. M Payami, *J. Phys.:Condens. Matter* **13** (2001) 4129.
10. W Kohn and L J Sham, *Phys. Rev.* **140** (1965) A1133.
11. J F Janak, *Phys. Rev. B* **18** (1978) 7165.
12. C Fiolhais and J P Perdew, *Phys. Rev. B* **45** (1992) 6207.
13. M Payami and N Nafari, *J. Chem. Phys.* **109** (1998) 5730.
14. A Kiejna, *Phys. Rev. B* **47** (1993) 7361.
15. M Seidl, J P Perdew, M Brajczewska and C Fiolhais, *Phys. Rev. B* **55** (1997) 13288.

Acknowledgement:

The author would like to thank Bahram Payami for providing computer facilities.